Longitudinal Uniformity of Commercial Bi2223 Tapes Characterized by Scanning Hall-Probe Microscopy

Ryoji Inada, Shohei Baba, Ryosuke Ohtsu, Tomohide Makihara, Shusaku Sakamoto, and Akio Oota

***Abstract*—We investigated remanent field distributions for commercial Bi2223 tapes with length of 1 m and high critical current I_c of 150 A (77 K, self-field) developed by Sumitomo Electric Industries (SEI) Ltd., by scanning Hall-probe microscopy (SHM) with an active area of 50 μm × 50 μm. All tapes are prepared by powder-in-tube process and sintered by controlled-over pressure (CT-OP) processing at final sintering stage. A bare tape and a 3-ply reinforced one with stainless tape laminations were used for measurements. The distribution of remanent field B_{rz} in perpendicular to broader face of a magnetized tape was measured using SHM, at a fixed distance of 0.5 mm away from a tape surface. Although absolute B_{rz} values in a reinforced tape were 10% lower than bare one, the shape of B_{rz} profile along a lateral direction of a tape was hardly affected by reinforcement and uniformly distributed along a length of each tape. Moreover, we cut away 15 cm piece sample from each tape and measured B_{rz} profile before and after double-sided bending with a bending diameter of 30 mm. The results indicated that degradation in both intensity and longitudinal uniformity of B_{rz} for a reinforced tape is much smaller than for a bare one.**

***Index Terms*—Bi2223 tapes, remanent field, Hall-probe, longitudinal uniformity**

I. Introduction

SILVER sheathed $Bi_2Sr_2Ca_2Cu_3O_x$ (Bi2223) high temperature superconducting (HTS) tapes are one of the most promising candidates for realization of HTS power devices such as cables and electric motors. Recently, critical current property of Bi2223 tapes has been greatly improved by applying controlling over pressure (CT-OP) processing at final sintering stage during tape fabrication [1], [2], which was developed by Sumitomo Electric Industries (SEI) Ltd. The conditions of temperature and oxygen partial pressure in CT-OP process were adjusted to enhance the critical current density. At present state, critical current I_c for conventional 4 mm-width tape has attained to the level more than 200 A at 77 K and self-field. In addition, mechanical strength of a tape is greatly improved by metallic tape laminations such as stainless steel and Cu-alloy [1]–[3]. This has been mainly confirmed by transport critical current I_c measured by a conventional DC four-probe method. However, transport I_c represents only averaged property between a pair of voltage taps on a tape and seems to be insufficient to examine the influence of mechanical deformation on longitudinal uniformity of transport property for a tape. Therefore, multi-sided characterization of tape uniformity should be strongly desired for quality control and further improvements of tape performance.

Scanning Hall-probe Microscopy (SHM) is a tool utilized in industry for magnetic and non-destructive evaluation of a variety of structural materials, such as stainless steel and low carbon steel [4], [5]. Moreover, SHM has been also applied to characterization of Bi2223 monocore or multifilamentary tapes [6]–[11] or YBCO coated conductors [12], [13]. In this paper, remanent field distributions for commercial Bi2223 tapes produced by SEI were evaluated using SHM. All tapes used for measurement are prepared by conventional powder-in-tube process and sintered by CT-OP processing at final sintering stage. A bare tape and a 3-ply reinforced one with stainless tape laminations were used for measurements. The results for both tapes were compared each other and influence of reinforcement on remanent field profile and their longitudinal uniformity of tape was studied.

TABLE I Specifications of commercial Bi2223 tapes with or without stainless tape laminations.

Tape Type	Type H	Type HT
Reinforcement	None	Stainless tapes (20 μm)
Tape cross section	4.20 mm × 0.23 mm	4.50 mm × 0.31 mm
Tape length	1 m	1 m
Averaged I_c (at 77 K, 0 T)	149 A	145 A
Standard deviation of I_c (at 77 K, 0 T)	0.7%	0.9%
Averaged $B_{rz\text{-}max}$	12.5 mT	11.6 mT
Standard deviation of $B_{rz\text{-}max}$	2.3%	2.9%

II. Experimental

Two CT-OP processed Bi2223 tapes produced by SEI were used as samples. One is a bare tape (Type H) and another is a 3-ply one laminated with 20 μm stainless tapes (Type HT) to improve mechanical strength and flexibility. Specifications of these tapes are summarized in Table 1. It is noted that Type HT

Manuscript received 3 August 2010. This work was supported in part by Grant-in-Aids for Scientific Research from MEXT (No.20686020) and JSPS (No.22560270) of Japan. It was also supported in part from TEPCO Research Foundation, Research Foundation for the Electrotechnology of Chubu (No.R-20302) and DAIKO Foundation. All Bi2223 tapes used for measurement were supplied by courtesy of Sumitomo Electric Industries Ltd.

R. Inada, S. Baba, R. Ohtsu, T. Makihara and A. Oota are with Toyohashi University of Technology, 1-1 Hibarigaoka, Tempaku-cho, Toyohashi, Aichi 4418580 Japan (e-mail: inada@ee.tut.ac.jp).

S. Sakamoto is with Kisarazu National College of Technology, 2-1-1 Kiyomidai-Higashi, Kisarazu, Chiba 2920041, Japan.

was prepared from same lot for bare one Type H. Lengths of both tapes are 1 m. Before measuring remanent field, critical currents I_c at 77 K and self-field were measured at every 10 mm section along a length of each tape, by a conventional DC four probe method with an electric field criterion of 1 μV/cm. For measuring longitudinal I_c distributions without soldering voltage taps on a tape, contact-type voltage taps with a separation of 10 mm were used [11].

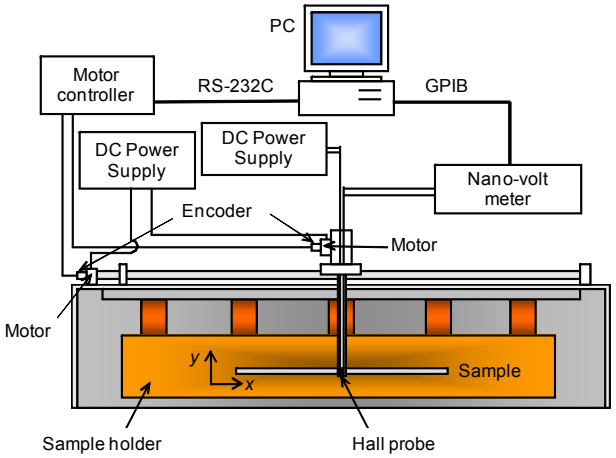

Fig. 1. A block diagram of scanning Hall-probe microscopy (SHM). An active area of the Hall-probe is 50 μm × 50 μm. The lift-off between the probe and the sample surface is approximately 0.5 mm.

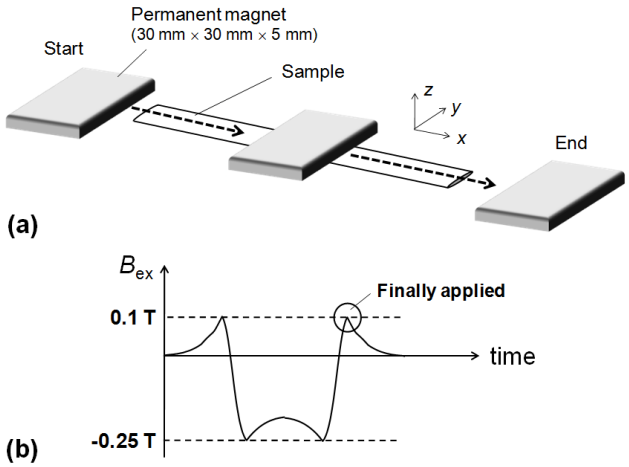

Fig. 2. Schematic diagrams for (a) magnetization method of a tape sample with using a rectangular permanent magnet with a size of 30 mm × 30 mm × 5 mm and (b) the change of applied field at an arbitrary longitudinal position x of a tape sample during the magnetization.

Two-dimensional distribution of remanent field B_{rz} in perpendicular to broader face of each tape was measured by Scanning Hall-probe microscopy (SHM) [5], [6]. Fig. 1 shows a block diagram for SHM. SHM was equipped with a micro-Hall probe with an active area of 50 μm × 50 μm on a movable x-y stage and a sample holder facing the probe. The probe was used to detect magnetic field in perpendicular to tape surface. After a tape was fixed on the sample holder at 77 K and zero fields, an external field B_{ex} was applied in perpendicular to tape surface. In order to magnetize a tape with its length of 1 m, a rectangular shaped permanent magnet with a size of 30 mm × 30 mm × 5 mm was placed on the tape surface, and then it was moved along a tape length (Fig. 2(a)) [10], [11]. As shown in Fig. 2(b), finally applied B_{ex} at an arbitrary position x along a tape length is estimated to be ~0.1 T, which is much higher than full-penetration field B_p of both tapes. Therefore, both tapes are expected to be in a critical state after removing B_{ex} [6], [8]–[11]. The Hall voltages were measured with a nanovoltmeter by scanning the probe on x-y stage with finite steps of 0.2 mm in both longitudinal (x) direction and lateral (y) direction, at a distance of 0.5 mm away from tape surface. Consequently, B_{rz} distributions on a tape can be visualized two-dimensionally.

Firstly, we measured B_{rz} distributions on 1 m-long tapes with or without reinforcement to check the influence of lamination process for metallic tapes on longitudinal tape uniformity. Then, we cut away 150 mm piece from each tape and measured B_{rz} profiles before and after applying double-sided bending at room temperature. A schematic diagram for double bending test is shown in Fig. 3. For the bending, tape was wound by hand on a cylindrical former with a diameter of 30 mm. It is noted that each tape was subsequently flattened after the bending for B_{rz} measurement by SHM.

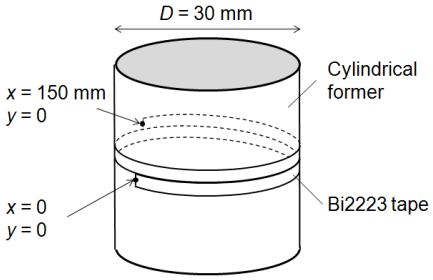

Fig. 3. A schematic diagram for double-sided bending test of tape sample. Bending diameter for our experimental was set to be 30 mm.

III. Results and Discussion

Averaged values and standard deviations for transport critical currents I_c (77 K, self-field) measured at every 10 mm section along a length of each tape are summarized in Table 1. Although averaged I_c for reinforced tape Type HT are ~3% lower than bare one Type H, the longitudinal uniformity was confirmed to be within 1% for both tapes.

Fig. 4 shows the remanent field B_{rz} distributions on a both tapes. In both graphs, x corresponds to longitudinal position while y does lateral one for each tape. For the readability of B_{rz} profiles, y-axis in each data is enlarged in actual size. In lateral direction for both tapes, it is confirmed that a strong positive peak of B_{rz} was detected near a tape center (y = 0 mm), while B_{rz} shows small negative peaks near both tape edges ($|y|$ = 2 mm). This specific lateral B_{rz} profile is uniformly distributed along a length of each tape. By addressing both I_c and B_{rz} measurement, stainless tape laminations for the reinforcement have no side effect on longitudinal uniformity of tape property.

According to critical state model, the magnitude of B_{rz} at an arbitrary longitudinal position x strongly correlates to critical current density J_c at x if the transverse cross-sectional geometry was uniform along a tape length [10]. By addressing this fact, we defined the maximum peak of B_{rz} in a lateral direction of a tape as a parameter $B_{rz\text{-}max}$, and longitudinal distributions of $B_{rz\text{-}max}$ for both tapes were compared in Fig. 5. Averaged values

and standard deviations for $B_{rz\text{-}max}$ at measurement section of transport I_c are also listed in Table 1. As can be seen, Type HT with stainless tape laminations has 7–8% lower $B_{rz\text{-}max}$ than Type H without reinforcement. The difference in $B_{rz\text{-}max}$ among the tapes is larger than that in I_c (< 3%) as shown in Table 1. This is mainly attributed to the increase in actual distance between filamentary core in a tape and the probe by stainless tape laminations. Since total thickness for Type HT with stainless tape laminations is 80 μm larger than tape Type H without reinforcement, the distance from filamentary core and the probe would be increased by ~40 μm in Type HT.

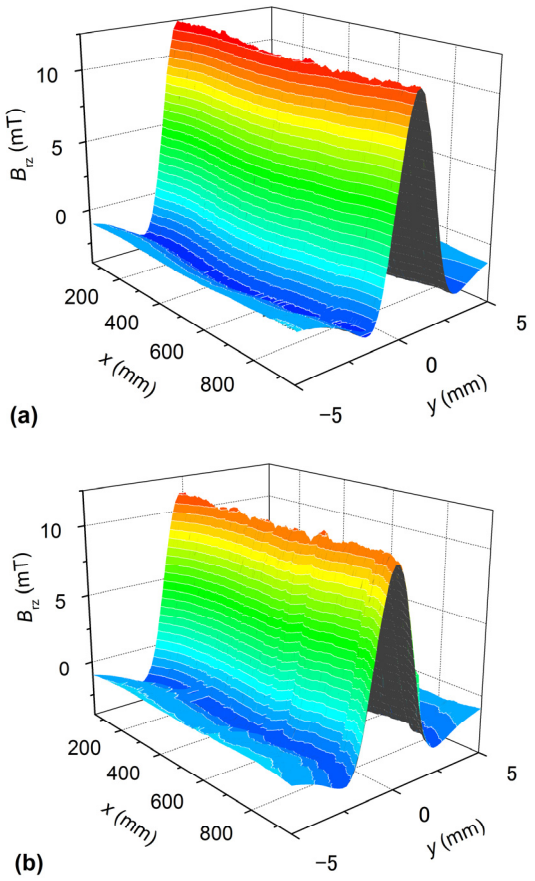

Fig. 4. Distributions of remanent field B_{rz} at 77 K in perpendicular to broader face of Bi2223 tape: (a) Type H without reinforcement and (b) Type HT reinforced with 20 μm stainless tape laminations. x corresponds to the position parallel to the tape length while y does the position parallel to the tape width.

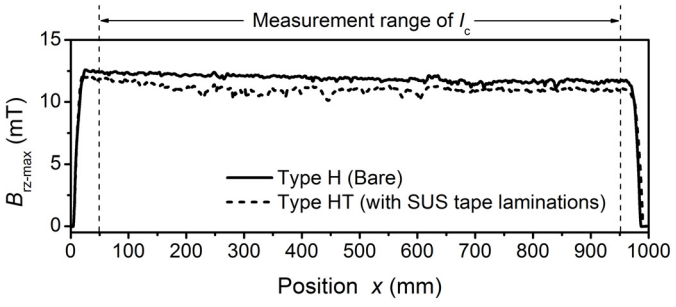

Fig. 5. Longitudinal distributions for parameter $B_{rz\text{-}max}$ at 77 K for Type H without reinforcement and Type HT reinforced with 20 μm stainless tape laminations. Averaged values and standard deviations for $B_{rz\text{-}max}$ at I_c measurement region are summarized in Table 1.

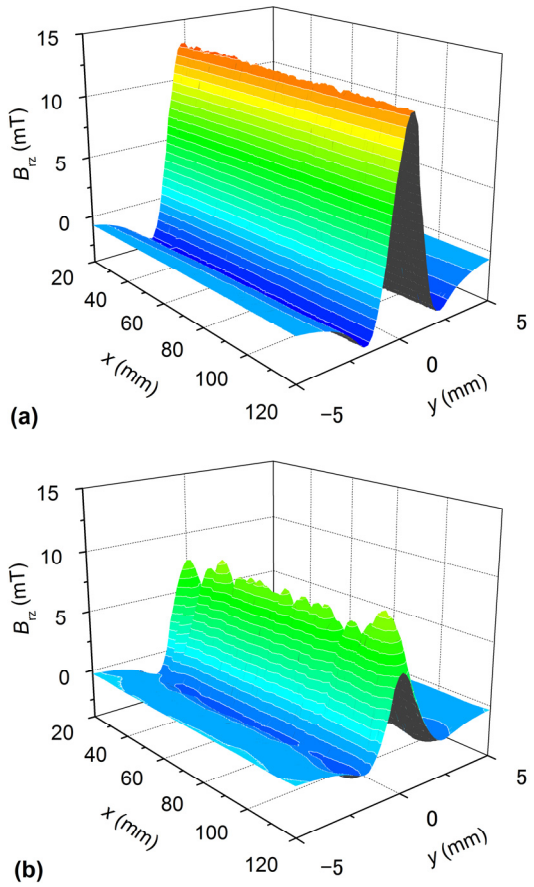

Fig. 6. Distributions of remanent field B_{rz} at 77 K in perpendicular to broader face of Type H without reinforcement: (a) before bending and (b) after bending. Double-sided bending was done at room temperature with its diameter of 30 mm. Note that x = 0 and 150 mm (not shown in both graphs) correspond to both tape ends (see Fig. 3).

Although the uniformity of $B_{rz\text{-}max}$ is nearly the same among the tapes, the standard deviations for $B_{rz\text{-}max}$ are 2–3 times larger than those for I_c measured at every 10 mm section. It should be noted that I_c represents macroscopic properties averaged between the voltage taps separations so that it does not show longitudinal non-uniformity in detail. On the other hand, B_{rz} in Figs. 4 and 5 was measured at every 0.2 mm step along a tape length so that they can represent longitudinal non-uniformity of tape property more precisely. Therefore, the difference in uniformity for $B_{rz\text{-}max}$ and I_c is mainly attributed to the difference in resolutions for both measurements.

Next we discuss B_{rz} distribution for Bi2223 tape before and after the double-sided bending with a bending diameter of 30 mm. Fig. 6 shows the distributions of B_{rz} on Type H without reinforcement before and after the bending. It should be noted that each tape is positioned at x = 0 to 150 mm. As can be seen, the magnitude of B_{rz} on a tape was significantly reduced by bending. Since the magnitude of B_{rz} is proportionate to critical current density J_c if cross sectional geometry are identical along a tape length, reduction of B_{rz} suggests J_c deterioration by bending. Longitudinal $B_{rz\text{-}max}$ distributions for Type H and Type HT measured before and after the bending are compared in Fig. 7. As can be seen, the reduction of $B_{rz\text{-}max}$ after bending for Type HT with reinforcement is smaller than Type H without reinforcement. This is consistent with I_c measurements after the bending test reported in [1]. In addition, it should be mentioned

that the bending caused degradation in not only $B_{rz\text{-}max}$ intensity but also its longitudinal uniformity. This strongly suggests that longitudinal non-uniformity of transport property was significant degraded by bending. The fluctuation of $B_{rz\text{-}max}$ after the bending in Type H is more remarkable than in Type HT.

At positions x = 30 and 120 mm in Type H, two sharp minima of $B_{rz\text{-}max}$ are clearly observed after the bending (Fig. 7(a)). Surprisingly, the small minima of $B_{rz\text{-}max}$ are also confirmed in Type HT after the bending at nearly the same positions (Fig. 7(b)). Although the reason why $B_{rx\text{-}max}$ was significantly degraded at these specific points is not clear at present, it might be attributed to our bending method shown in Fig. 3. Moreover, as shown in Fig. 7 (a), Type H shows a very narrow minimum before the bending at x = 32 mm. This happens to nearly coincide with the sharpest minimum in the curve after the bending. This may show the possibility that the bending significantly worsened a defect that was previously present in a tape. Type HT also shows a similar narrow minimum before the bending at x = 110 mm (Fig. 7(b)), but there is no sharp minimum at this position after the bending. This might be due to mechanical strengthening by stainless tape laminations. We are speculating that a sharp degradation of $B_{rx\text{-}max}$ similar with Type H is observed if we bent Type HT with smaller bending diameter.

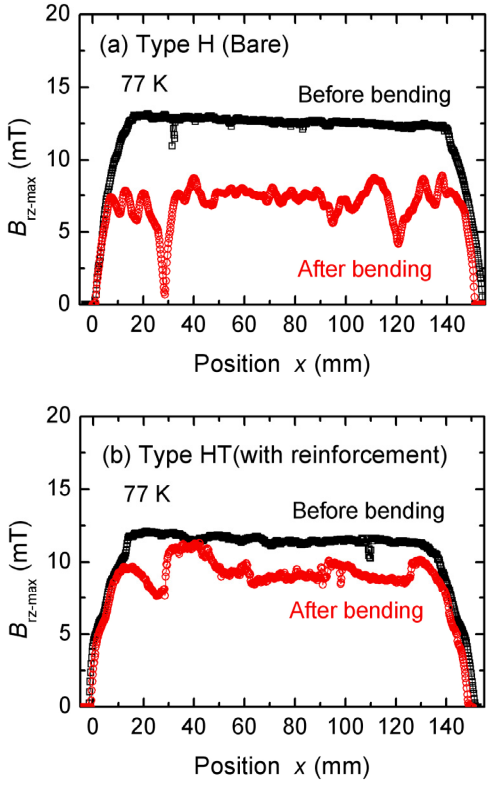

Fig. 7. Longitudinal distributions for $B_{rz\text{-}max}$ before and after double bending test with a bending diameter of 30 mm: (a) Type H without reinforcement and (b) Type HT with 20 μm stainless tape laminations. Note that each tape is positioned at x = 0 to 150 mm in graphs.

IV. Conclusion

Using scanning Hall-probe microscopy (SHM) with an active area of 50 μm × 50 μm, we investigated remanent field distributions on commercial Bi2223 tapes developed by Sumitomo Electric Industries Ltd. 1 m long commercial Bi2223 tapes with or without reinforcement by 20 μm stainless tape laminations were used as samples. Although the intensity of remanent field B_{rz} on a reinforced tape was slightly reduced by increase the distance between filamentary core and the probe, both B_{rz} profile along a lateral direction and its longitudinal uniformity are hardly affected by stainless tape laminations. The longitudinal uniformity of maximum B_{rz} near the tape center is confirmed to be within 3% in both tapes. After the double-sided bending with a bending diameter of 30 mm, the degradation of both intensity and longitudinal uniformity of B_{rz} in a reinforced tape are greatly suppressed compared with a bare one. Although further study to examine the effect of bending on the degradation in longitudinal uniformity of tapes is necessary, these results strongly suggest that our measurement method with SHM is very useful to characterize the longitudinal non-uniformity of tapes simply and non-destructively.

References

[1] N. Ayai, S. Kobayashi, M. Kikuchi, T. Ishida, J. Fujikami, K. Yamazaki, S. Yamade, K. Tatamidani, K. Hayashi, K. Sato, H. Kitaguchi, H. Kumakura, K. Osamura, J. Shimoyama, H. Kamijyo, and Y. Fukumoto, "Progress in performance of DI-BSCCO family," *Physica C* 468, pp. 1747-1752, 2008.

[2] N. Ayai, K. Yamazaki, M. Kikuchi, G. Osabe, H. Takaaze, H. Takayama, S. Kobayashi, J. Fujikami, K. Hayashi, K. Sato, K. Osamura, H. Kitaguchi, S. Matsumoto, T. Kiyoshi, and J. Shimoyama, "Electrical and mechanical properties of DI-BSCCO Type HT reinforced with metallic sheathes," *IEEE Trans. Appl. Supercond.* 19, pp. 3014-3017, 2009.

[3] K. Osamura, S. Machiya, H. Suzuki, S. Ochiai, H. Adachi, N. Ayai, K. Hayashi, and K. Sato, "Improvement of reversible strain limit for critical current of DI-BSCCO due to lamination technique," *IEEE Trans. Appl. Supercond.* 19, pp. 3026-3029, 2009.

[4] A. Oota, T. Ito, K. Kawano, D. Sugiyama, and H. Aoki, "Magnetic detection of cracks by fatigue in mild steels using a scanning Hall-sensor microscope," *Rev. Sci. Instrum.* 70, pp.184-186, 1999.

[5] A. Oota, K. Kawano, K. Miyake, T. Ito, D. Sugiyama, and H. Aoki, "Visualization of strain-induced phase breakdown in austenite stainless steel using a scanning Hall-sensor microscope," *Jpn. J. Appl. Phys.* 41, pp. 5463-5466, 2002.

[6] K. Kawano and A. Oota, "A study on self-field distribution in Ag-sheathed $(Bi,Pb)_2Sr_2Ca_2Cu_3O_x$ monofilamentary tape using a scanning Hall sensor magnetometry," *Physica C* 275, pp. 1-11, 1997.

[7] A. Oota, K. Kawano, and T. Fukunaga, "Self fields and current distribution due to DC transport currents on Ag-sheathed $(Bi,Pb)_2Sr_2Ca_2Cu_3O_x$ tapes," *Physica C* 291, pp. 188-200, 1997

[8] A. Oota, K. Kawano, and K. Yagi, "Microstructure and transport current path in Ag-sheathed $(Bi,Pb)_2Sr_2Ca_2Cu_3O_x$ monofilamentary tapes rolled at different pressures," *Ceramics International* 26, pp. 663-668, 2000.

[9] J. Kvitkovic and M. Polak, "Remanent magnetization in multifilamentary Bi-2223 tapes with filament bridging," *Physica C* 372-376, pp. 1012-1015, 2002.

[10] S. Baba, R. Inada, T. Makihara, Y. Nakamura, A. Oota, S. Sakamoto, C.S. Li, and P.X. Zhang, "Evaluation of remanent field distributions on Bi2223 tapes with oxide barriers by using scanning Hall-probe microscopy," *J. Phys. Conf. Ser.* 234, p.022004, 2010.

[11] R. Inada, T. Makihara, Y. Araki, S. Baba, Y. Nakamura, A. Oota, S. Sakamoto, C.S. Li, and P.X. Zhang, "Non-destructive evaluation of longitudinal uniformity for twisted Bi2223 tapes using scanning Hall-probe microscopy," *Physica C* 470, pp. 1392-1396, 2010..

[12] P. Usak, M. Polak, and P. Mozola, "Measurement of lateral transport current distributions in YBCO tape," *IEEE Trans. Appl. Supercond.* 19, pp. 2839-2842, 2009.

[13] M. Inoue, K. Abiru, Y. Honda, T. Kiss, Y. Iijima, K. Kakimoto, T. Saitoh, K. Nakao, and Y. Shiohara, "Observation of current distribution in high-Tc superconducting tape using scanning Hall-probe microscope," *IEEE Trans. Appl. Supercond.* 19, pp.2847-2850, 2009.